



LAWRENCE
LIVERMORE
NATIONAL
LABORATORY

Application of Modern Autoradiography to Nuclear Forensic Analysis

T. Parsons-Davis, K. Knight, M. Fitzgerald, G.
Stone, L. Caldeira, C. Ramon, M. Kristo

July 28, 2017

Forensic Science International

Disclaimer

This document was prepared as an account of work sponsored by an agency of the United States government. Neither the United States government nor Lawrence Livermore National Security, LLC, nor any of their employees makes any warranty, expressed or implied, or assumes any legal liability or responsibility for the accuracy, completeness, or usefulness of any information, apparatus, product, or process disclosed, or represents that its use would not infringe privately owned rights. Reference herein to any specific commercial product, process, or service by trade name, trademark, manufacturer, or otherwise does not necessarily constitute or imply its endorsement, recommendation, or favoring by the United States government or Lawrence Livermore National Security, LLC. The views and opinions of authors expressed herein do not necessarily state or reflect those of the United States government or Lawrence Livermore National Security, LLC, and shall not be used for advertising or product endorsement purposes.

Application of Modern Autoradiography to Nuclear Forensic Analysis

Tashi Parsons-Davis,¹ Kim Knight,¹ Marc Fitzgerald,^{1,2} Gary Stone,¹ Lee Caldeira,¹ Christina Ramon,¹ Michael Kristo¹

¹Lawrence Livermore National Laboratory, Livermore, CA

²University of Nevada, Las Vegas

Key words: Nuclear forensics, autoradiography, radioactivity, imaging

Abstract

Modern autoradiography techniques based on phosphorimaging technology using image plates (IPs) and digital scanning can identify heterogeneities in activity distributions and reveal material properties, serving to inform subsequent analyses. Here, we have been adopted these advantages for applications in nuclear forensics. IP autoradiography is a relatively simple, non-destructive method for sample characterization that records an image reflecting the relative intensity of alpha and beta emissions from a two-dimensional surface. Such data are complementary to information gathered from radiochemical characterization via bulk counting techniques, and can guide the application of other spatially resolved techniques such as Scanning Electron Microscopy (SEM) and Secondary Ion Mass Spectrometry (SIMS). IP autoradiography can image large 2-dimensional areas, with relatively low detection limits for actinides and fission product decay, and sensitivity to a wide dynamic range (10^5) of activity density in a single image. Distributions of radioactivity in nuclear materials can be generated with a spatial resolution of approximately 50 μm using IP autoradiography and digital scanning. While the finest grain silver halide films still provide the best possible spatial resolution (down to $\sim 10 \mu\text{m}$), IP autoradiography has distinct practical advantages such as shorter exposure times, no chemical post-processing, reusability, rapid plate scanning, and automated image digitization. Sample preparation requirements are minimal, and the analytical method does not consume or alter the sample. These advantages make IP autoradiography ideal for routine screening of nuclear materials, and for the identification of areas of interest for subsequent micro-characterization methods. In this paper we present a summary of our setup, as modified for nuclear forensic sample analysis and related research, and provide examples of data from select nuclear fuel cycle samples and historical nuclear test debris.

Introduction

The spatial distribution of radioactivity in nuclear materials, samples contaminated with radioactive materials, or historical nuclear test debris preserves indications of physical and chemical processes affecting the formation or modification of the sample. Characterization of the intensity and relative distribution of activity in these types of nuclear and radioactive materials thus supports analysis and research to understand the formation and history of these materials. While autoradiography has been used in the past as a non-destructive method of radioactive sample characterization, the historical requirements for autoradiography, including post-imaging chemical processing of the films, limited adoption of the technique in modern applications. Here, we present a set of methods and demonstrate

the application and advantages of these methods for rapid, straightforward triage and characterization of samples such as those encountered in nuclear forensic investigations and related nuclear materials research.

Autoradiography is the practice of creating an image of a radioactive source by the direct exposure of imaging media. Autoradiography is the oldest technique for detecting radioactivity, and was extensively developed throughout the 20th century for application in the physical and life sciences.¹ The image is created by the deposition of energy into an emulsion, causing a chemical excitation where the energy deposited. Traditional autoradiography uses film emulsions, silver halide film being the most common. Radiation incident to silver halide crystals promotes halide electrons from the valence to the conduction band, where they are free to move throughout the crystal. The electrons then get trapped in a lower energy state at defect or impurity sites, where they attract and reduce surrounding silver ions.² Amplification of latent images is achieved through chemical development of silver grains. The resolution of this imaging system is strongly dependent on the thickness of the emulsion, the size of the silver halide grains dispersed in the emulsion, the optical densitometer performance, and the strength of the development process.

Phosphor image plate (IP) technology was initially developed by Fuji film in the early 1980's to provide an alternative to conventional X-ray film for diagnostic radiography.³ The high sensitivity, accuracy, efficiency and convenience of phosphor imaging soon found application in X-ray diffraction and scattering experiments, and autoradiography.⁴ In IP systems, barium fluorohalide crystals doped with europium activator (BaFX:Eu²⁺; X = Cl, Br, I) are the photosensitive grain, and the image is formed via photostimulated luminescence (PSL). Incident radiation oxidizes the Eu²⁺ to Eu³⁺, promoting electrons to the conduction band and producing the latent image. Electrons are trapped in fluorohalide vacancies, called F-centers, until they are stimulated by laser light to return to the Eu³⁺ activator.⁵ This transition releases characteristic light, which is detected by a photomultiplier tube. As with film, resolution is a function of emulsion thickness, grain size, optical readout system, and the properties of the sample being imaged .

Autoradiography has been used extensively in medical and biological research,^{1,6-8} as well as in geology,^{9,10} nuclear physics^{2,11} and microscopy.^{12,13} Since the 1950's, autoradiography has also been a valuable tool in the analysis of fallout and crater glass in nuclear explosions. Early research on fallout from the Pacific Proving Grounds and Nevada Test Site^{14,15} used autoradiography to understand activity distributions in post-detonation materials, and these observations were instrumental to the development of the first theories of fallout formation and radioisotope fractionation. During the nuclear test program, debris samples were exposed to imaging media soon after the shot occurred, thus many autoradiographs were saturated from exposure to short-lived fission products. In modern fallout research autoradiography has been shown to be a useful tool to locate residual fuel and other long-lived radioactive components in historic nuclear debris. Autoradiography has been applied qualitatively as part of multi-method analysis of trinitite¹⁶⁻¹⁸ and of debris from a U fueled test.¹⁹

Another ideal application for characterization of radioactivity distributions in nuclear materials is nuclear forensics, the technical analysis of radioactive or nuclear materials found outside of legal control

to provide data related to provenance, production history, and trafficking route for the sample.²⁰ Through application of diverse array of analytical techniques, relevant databases, and expertise, analysis and interpretation of nuclear forensic data may be combined with law enforcement information to aid in the association of illicit nuclear or radioactive material with a source. Typical material properties characterized for technical nuclear forensic analysis may include physical properties (*e.g.*, appearance, form, weight, density, grain size, etc.), chemical and isotopic composition, concentrations of trace elements, identity and concentration of trace radionuclides from fission or neutron activation, and the production date or date of last chemical separation. Many of the analytical methods useful to nuclear forensics tend to be resource and labor intensive, however. In addition, primary samples can often be made up of more complex mixtures of starting materials, necessitating an understanding of spatial relationships to provide comprehensive characterization of the sample. The application of screening methods such as autoradiography to triage samples requiring further analysis can enable more effective use of resources and guide analytical planning of follow on analyses.

In a nuclear forensic investigation, decisions regarding sequencing of analyses must be carefully planned to minimize any contamination or compromise of the sample, and, in the cases where there are limited quantities of the sample, to make the most effective use of the material. For these reasons, it is often advantageous to perform non-destructive analytical techniques, *i.e.*, those that do not use or alter the sample, prior to any destructive analysis. Because it is usually the radiological properties of the material that warrant a nuclear forensic investigation, one of the most common initial screening techniques is gamma counting of the bulk sample, as received. While this method provides information on the bulk characteristics of sample radioactivity, it cannot be used to determine activity distributions, or to establish if select portions of a material may be of higher interest for subsequent characterization. For example, evidence of radioactive contamination limited to a sample surface in contrast to evidence of radioactivity throughout the volume of a material may impact decisions regarding further analytical interrogation. If sample radioactivity is dominated by surface contributions, dissolution-based methods used to characterize the radioactive isotopes may choose to focus on these surfaces, to minimize the addition of unnecessary background into the chemical separations. Alternately, assessment of a volumetric activity distribution may indicate that selection of a representative volume of the material will provide better characterization of the material and its radioisotope inventory and properties.

For some nuclear materials, the primary sample may be too large or otherwise warrant sub-aliquoting. For example, many types of spatially resolved microanalysis such as electron microscopy, X-ray microanalysis with energy dispersive or wavelength dispersive X-ray spectroscopy (EDS or WDS), spatially resolved infrared (FTIR) and Raman spectroscopies may be considered as part of a nuclear forensic investigation, particularly if some degree of structural or compositional heterogeneity is present.²¹ Scanning electron microscopy (SEM) and transmission electron microscopy (TEM) provide imaging with nm and sub-nm spatial resolution, respectively, and can be coupled with EDS or WDS to provide elemental composition data in nuclear forensic samples. Recently the focused ion beam technique has been incorporated to expand electron imaging of nuclear forensic samples to 3 dimensions.²² Spectroscopies in the lower energy regimes such as FTIR and Raman provide molecular information, and can be applied to individual μm -sized particles.²³ Most of these spatially resolved

techniques will not detect trace radioactive contaminants such as actinides, fission, or activation products, however, necessitating additional guidance if the areas of radioactivity are of highest interest. For spatially resolved methods able to quantify trace radioactivity, such as laser-ablation inductively coupled plasma mass spectrometry (LA-ICP-MS), resonance ionization mass spectrometry (RIMS), and secondary ion mass spectrometry (SIMS), non-destructive screening by a method such as autoradiography can reveal the distribution of radioactivity in the entire sample and/or within sub-aliqouts of the sample, aiding efficient targeting of analyses. In this paper, we utilize digital imaging plates, as well as a laser plate scanning system, to demonstrate how this very simple set of tools can provide fundamental information on the occurrence, relative intensity, and distribution of radioactivity within nuclear materials. We show how autoradiography can be incorporated as a non-destructive screening tool and characterization method for nuclear forensic analysis. We discuss the advantages and limitations of the method and its application, and several illustrative examples are presented.

Materials and Methods

Sample selection and preparation

While any material emitting detectable radioactivity can be imaged by autoradiography, the method is particularly useful for imaging the presence of beta emitters, and for alpha emitters on or near a sample surface. This is simply because the higher linear energy transfer of charged particles means their energy is deposited into a small area of the IP to create high image intensity near the emission of the particle. Alpha particles have the shortest range and can only be detected when emitted at or very near (within $\sim 30 \mu\text{m}$) the sample surface. Beta radiation may traverse up to a few mm of sample volume to reach the IP, depending on the particle energy and the sample material. Gamma and neutron radiation are much more penetrating, and can travel through several cm of sample volume to activate the IP, but create diffuse images due to less interaction with the emulsion. Fuji Film co. manufactures BAS-ND IPs that are doped with ^{203}Gd to increase neutron sensitivity. Limited information can be obtained from irradiated fuel and other high-activity samples because high activation of the IP by multiple radiation fields may mask heterogeneity in source distribution. In unirradiated uranium materials, areas of higher alpha activity can be identified amidst the more diffuse beta, gamma and X-ray produced image.

The best resolution images of activity distribution in solid samples, particularly when imaging alpha emitters, is achieved from imaging flat, smooth, 2-dimensional sample surfaces (also optimal for other spatially resolved methods such as SEM/EDS imaging and SIMS analysis). Preparation of sample surfaces for spatial analysis generally includes mounting in epoxy, and then polishing the exposed surface to a tolerance of $<1 \mu\text{m}$. No coating is needed for autoradiography, and overcoating of the sample surface will interfere with the transmission of activity (particularly alpha emitters). If subsequent analyses will require coating the sample surface (*e.g.*, in electron microscopy applications, where non-conductive samples are often coated with carbon or other conductive materials to reduce charging artifacts), the coating should be applied after the autoradiography is completed. Some degree of surface roughness can be tolerated, however, and 3-dimensional objects can also be characterized by autoradiography. For example, the relatively flat surfaces of conventional fuel pellets are conducive to

direct autoradiography, with no additional sample preparation, although the preparation of polished surfaces can improve image resolution. If a polished surface is not used for imaging, variations in the distance between the image plate and sample surface across the area of the sample creates artifacts in the spatial distribution of the intensity in the resulting image, and must be considered. The physical size of samples is limited only by the size of the image plates and digital scanner. In general, plates with overall dimensions of 20 x 40 cm are commercially available. We often cut or tailor IPs to relevant sample sizes.

To search soils or other particulate matter to isolate radioactive particles and the carriers of the activity present in the bulk sample, we use a method similar to Mukai et al.²⁴ A monolayer of the material is distributed onto a 10 cm x 15 cm Gel-Pak® adhesive pad with a 5.5 mm grid pattern (www.gelpak.com, X8 Gel-Pak Grid #P-0039) in preparation for imaging. The Gel-Pak substrate helps minimize movement of material during the analysis and handling, but does not bind to the sample. An important consideration, particularly in this application, is that it is often desirable to correlate the autoradiograph with the physical coordinates of the sample(s) so that subsequent identification of materials of highest interest or correlation with other spatial characterization imaging is possible. This can be particularly challenging for samples with sporadic radioactivity and collections of materials such as mixed soil samples. If image registration is needed, then the sample alignment with respect to the edges of the image plate must be controlled and documented so that relative orientation can be recreated. Deliberate deposition of radioactive markers to the sample setup, in alignment with the image plate can be used to indicate sample coordinates in the autoradiograph. Another convenient method is to place small blocks of Pb or other shielding material at intentional positions on the back of the IP during sample exposure. The blocks will shield the IP from background cosmic radiation, so their positions show up in the resulting image as areas with lighter background.

Autoradiography is also used to check homogeneity of sources prepared for analyses including alpha counting, or as nuclear reaction targets via electrodeposition of radionuclides from solution onto metal disks or stubs. Depending on the amount of material to be deposited, and the requirements of the film, these sources may be prepared with variations of molecular deposition²⁵ or electrodeposition from aqueous sodium sulfate-bisulfate solution.²⁶ In this case, the sources tend to be sufficiently flat as prepared, and no additional polishing or preparation is needed.

Contamination of the imaging plates by sample surfaces can occur, as direct contact of the plate and sample surface is generally desirable. Samples should be checked for dispersible contamination prior to imaging. Cross contamination of samples and artifacts due to contamination of the image plates should be monitored, and (as far as possible) avoided. A thin sheet of Mylar, or other disposable, protective film may be inserted between the image plate and the sample surface, with the caveat that alpha particles may be blocked by the protective layer and thus won't contribute to the image. Many nuclear forensics samples are non-dispersible and can be directly imaged without contaminating the IP. Image plate scans with no sample exposure should be done regularly to check the IPs, and most types already have a thin protective coating so they can be gently cleaned when necessary. When slightly diminished spatial resolution can be tolerated, samples such as electroplated alpha sources may be held a small distance away from the IP during imaging.

Autoradiography set up and sample exposure

To obtain the best possible resolution, it is important to maintain a stable sample configuration during exposure to image plates such that door and foot traffic, movement of the imaging tent, or minor earthquakes and construction will not shift the sample relative to the plate. This is particularly important for low activity samples requiring prolonged exposure times (days to weeks). Samples containing non-dispersible radioactivity can be held in direct contact with the image plate. This can be most simply achieved by placing the IPs on top of samples, emulsion side down, with a weight on top in a Harrison 1000 light-tight Pup tent (or similar).

If multiple samples are being imaged together (to provide comparative intensity information), however, this method requires that the samples be the same thickness and have two parallel sides. To accommodate wider variation in sample dimensions, we designed a custom IP exposure box to accommodate a range of samples prepared in the forms generally used for other types of spatially-resolved nuclear forensic analysis. This light-tight box, shown in Figure 1, uses magnets to align sample surfaces firmly in contact with the image plate in a stable configuration. Samples are mounted to aluminum pucks using double-sided foam tape, and these pucks are connected to screws that go through a hard-plastic block (machined from low-background acetyl resin) containing magnets. The screws allow each sample to be positioned individually to create a common plane of all the sample surfaces, regardless of thickness (see Figure 2). The IP is held emulsion side up in a fixed position at the bottom of the box. When the block is inserted, the block magnets are aligned with those in the sides of the box, forcing the sample surface plane to contact the IP. The flexibility of the foam tape accommodates small deviations from the condition that both sides of all samples be parallel. All samples should be photographed in the exposure configuration prior to imaging, and the operator must be acutely aware of the orientation of the image plate when it is transferred to the scanner.

When attempting to minimize contamination of IPs, slightly diminished spatial resolution is tolerated, and a physical separation is used between the sample surface and the IP. In our set up, we use a stainless-steel plate with 1 mm deep indents to hold 1" diameter disks in place, plated side up. Inside the Pup tent, the IP is then placed, emulsion side down, on top of the plate. A weight is placed on top to hold the image plate firmly in place without touching the radioactive sample surfaces.

In the case of soils or other particulate matter samples setup on Gel-Paks, we take a cut-to-size IP, and place it, emulsion-side down with a small weight on top. The Gel-Pak box lid is closed and the box is stored in the dark tent during exposure. The gel adhesive holds particles in place during exposure, but does not leave a residue that would interfere with further microanalysis. The location of "hot spots" in the image can then be correlated with the grid square for particle identification or down-selection.

Exposure times may range from a few minutes up to several weeks, depending on the concentration and specific activity of radioactive species in the samples. For most samples encountered in nuclear forensics, IP exposure times of 1 hour to 3 days yield high-quality images. Film autoradiography is less sensitive, and may require up to 10 times longer exposure times to produce a comparable image.^{4,27} The lower detection efficiency of film for ionizing radiation is mostly caused by ion

recombination along the charged particle tracks.² Film is also much more light-sensitive, so sample exposure must be completed in a specialized dark room, while semi-dark conditions are sufficient for IP autoradiography, as photons in the visible range are not energetic enough to promote the initial excitation, and are only avoided to minimize image fading during exposure.⁵

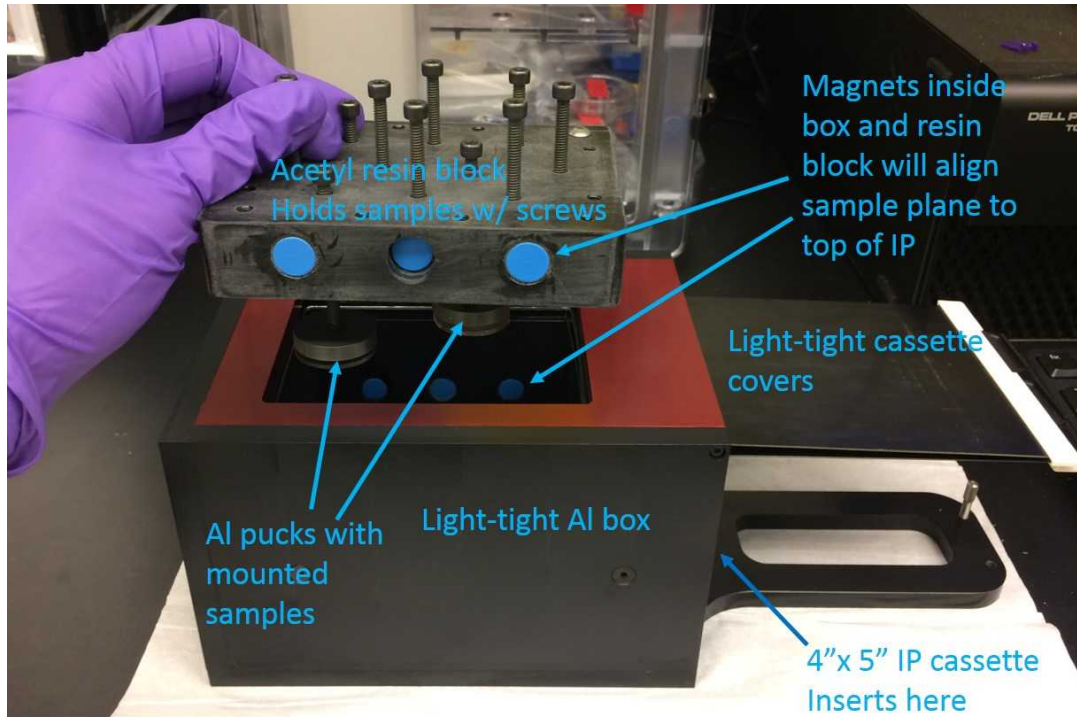


Figure 1: A custom made light-tight autoradiography sample exposure box (14.5 cm w x 19.2 cm l x 12.1 cm h) designed to for use with image plates.

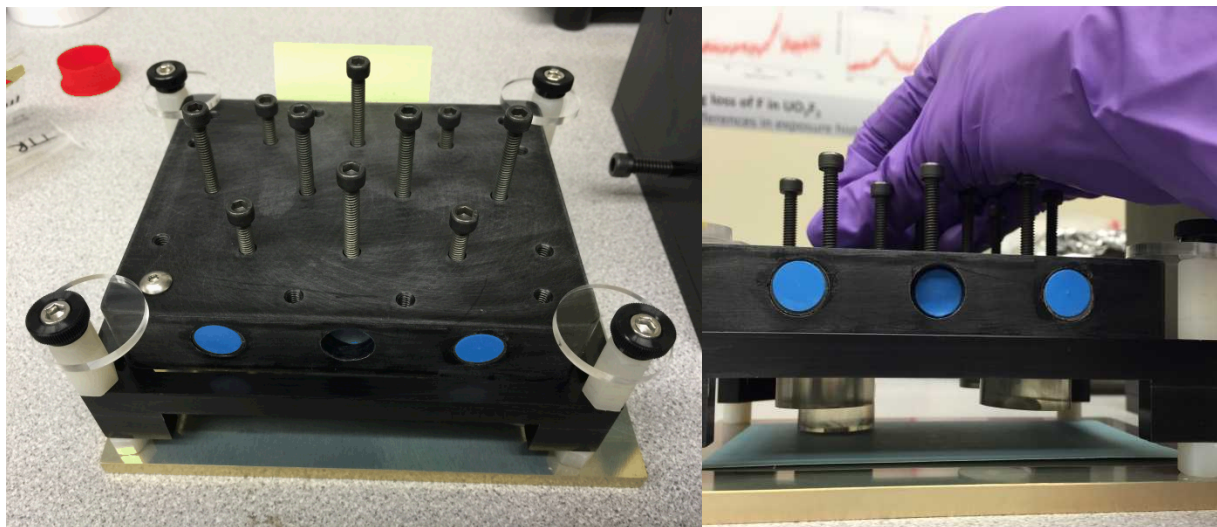


Figure 2: A stage is used to create a level plane at the appropriate distance from the magnets, for simultaneous imaging of multiple samples with variable dimensions. The samples are mounted to aluminum pucks with a temporary adhesive. The pucks are screwed in to the magnetized sample block, which will be placed inside the box. The sample block is 11.6 cm x 9.2 cm x 2.2 cm thick, and made of an acetyl resin (Delrin) that does not contribute background radiation. The magnets in the box (Fig. 1) and the block (here) are aligned to hold the samples flush to the image plate that is placed at the bottom of the box.

Phosphorimaging plates and processing

The image plates most routinely used are Fujifilm BAS-SR (super resolution) phosphor storage plates, with spatial resolution approximately 50 μm . These plates contain a 5 μm BaFBr sandwiched between a thin protective layer and a support film uniformly coated with Eu^{2+} . Following exposure, the digital image is collected with a GE Typhoon FLA 7000 scanner in phosphorimaging mode, with the dynamic range set to L5 and pixel size 25 μm . The photomultiplier tube (PMT) voltage is selected on a case-by-case basis, considering the expected sample activity and exposure time. The goal is to collect a high-quality image with enough intensity to view the activity distribution, but without saturated pixels. The PMTs are calibrated at least annually with a 50 μCi ^{14}C button source and a BAS-MS (multipurpose standard) phosphor storage plate, using the method of Williams et al.²⁸ Before reuse, IPs are placed in the GE FLA Image Eraser for at least 20 minutes. Other phosphor storage plates that can be used are BAS-ND for neutron detection, or BAS-TR, which are like BAS-MS plates, but without the protective film layer so that low-energy beta particles can be detected.

The scan voltage should be selected to optimize sensitivity to low activity regions without saturating pixels exposed to high activity regions, based on the exposure time and expected sample radioactivity. If there are saturated pixels in the first scan additional scans will remove image intensity until an image without saturated pixels is obtained. The Typhoon FLA 7000 saves images as .TIF images, which are scaled data and .Gel files, which contain the raw data that should be used for further analysis. There are a wide variety of image processing software that can be used to process and analyze the data. In our laboratory, we find the free software package ImageJ (<https://imagej.nih.gov/ij/index.html>) to be very useful and contain most of the needed image processing features. Lookup tables in ImageJ are used

to introduce false color to images, which can aid in visualization of distinguishable features and heterogeneity. Three-dimensional surface plots are also used to display individual features. Statistical analysis of raw pixel values informs the selection of radioactive features, and line plots are used for dimensional measurements. Other useful features include filters that create outline images or threshold images to find and identify particles.

Discussion of performance

Calibration considerations

IP autoradiography may be used qualitatively, and in some cases, semi-quantitatively. Calibration of the PMTs allows the selection of standardized, reproducible PMT voltages, and allows conversion of image gray values in each pixel to photo-stimulated level (PSL) values.²⁸ These PMT calibrations are necessary for numerical comparison among images scanned at different times, or on different scanners. For interpretation of new image data in context with older data from Fuji scanners, PMT voltages corresponding to one of the Fuji sensitivity values S1000, S4000, or S10000 should be used. This is generally not a concern in the relatively new field of nuclear forensics, but PMT calibrations must be maintained for general reproducibility and proper evaluation of data.

For applications that involve a single, known radionuclide, as in many medical and biological studies, a calibration curve can be constructed to correlate pixel intensity with activity density. This is usually not the case in nuclear forensics, which often involves samples containing mixed and/or unknown radionuclides. The practitioner should be mindful in interpreting autoradiographs, remembering that the image intensity in any area of the IP is proportional to the total energy deposited there by photons, neutrons, and charged particles. Due to the higher linear energy transfer of charged particles, they tend to dominate images created on general purpose or super resolution IPs. At low activity concentrations, image processing techniques have been developed to distinguish the radiation types based on the shape of individual particle tracks,²⁹⁻³¹ but at the higher activity concentrations usually encountered in nuclear and radioactive materials these methods may be impractical. In this case contributions from different particle emitters may be partially deconvoluted by imaging samples multiple times with various kinds of absorbers in between the sample surface and IP, however spatial resolution would suffer with increasing absorber thickness. Alpha particles can easily be blocked from contributing to the image, but many alpha emitters also emit X-ray or gamma rays that will penetrate the absorber and deposit energy into the IP. Other techniques that have been applied to differentiate radiation fields and particle energies include multi-layered emulsions, as well as photo-bleaching and multiple readout scans with different wavelengths used for photo-stimulation^{32,33} Although it would be possible to create a multivariate calibration curve for commonly encountered materials and obtain semi-quantitative information, at present, we find overall imaging of the activity distributions and their relative intensity in samples to be the most useful data.

Background and detection limits

High sensitivity to radioactive analytes is a strength of IP autoradiography relative to other spatially resolved analyses. With the most sensitive emulsions, and optimized exposure conditions

individual particles can be detected. In practice, the detection limits of individual radionuclides vary and may be determined by background conditions during exposure. The IP emulsion is sensitive to cosmic muons, thus underground laboratories and shielded exposure chambers may be beneficial. However, gamma and X-rays from ambient radiation sources also produce background. An example of typical detection limits is illustrated in Figure 3. An electroplated depleted uranium source with total alpha activity density of $3.69\text{E-}4$ Bq/mm² ($3.06\text{E}13$ atoms U/mm²) produced a latent image on a SR-type IP with a 24-hour exposure and maximum PMT voltage, while sources one order of magnitude less concentrated had activity density below the cosmic radiation flux, as evidenced by slightly less image intensity where the IP was shielded by the stainless-steel disk. Additional exposure time up to 120 hours did not produce images of sources below the 24-hour detection limit, but improved the image quality for those slightly above background activity densities.

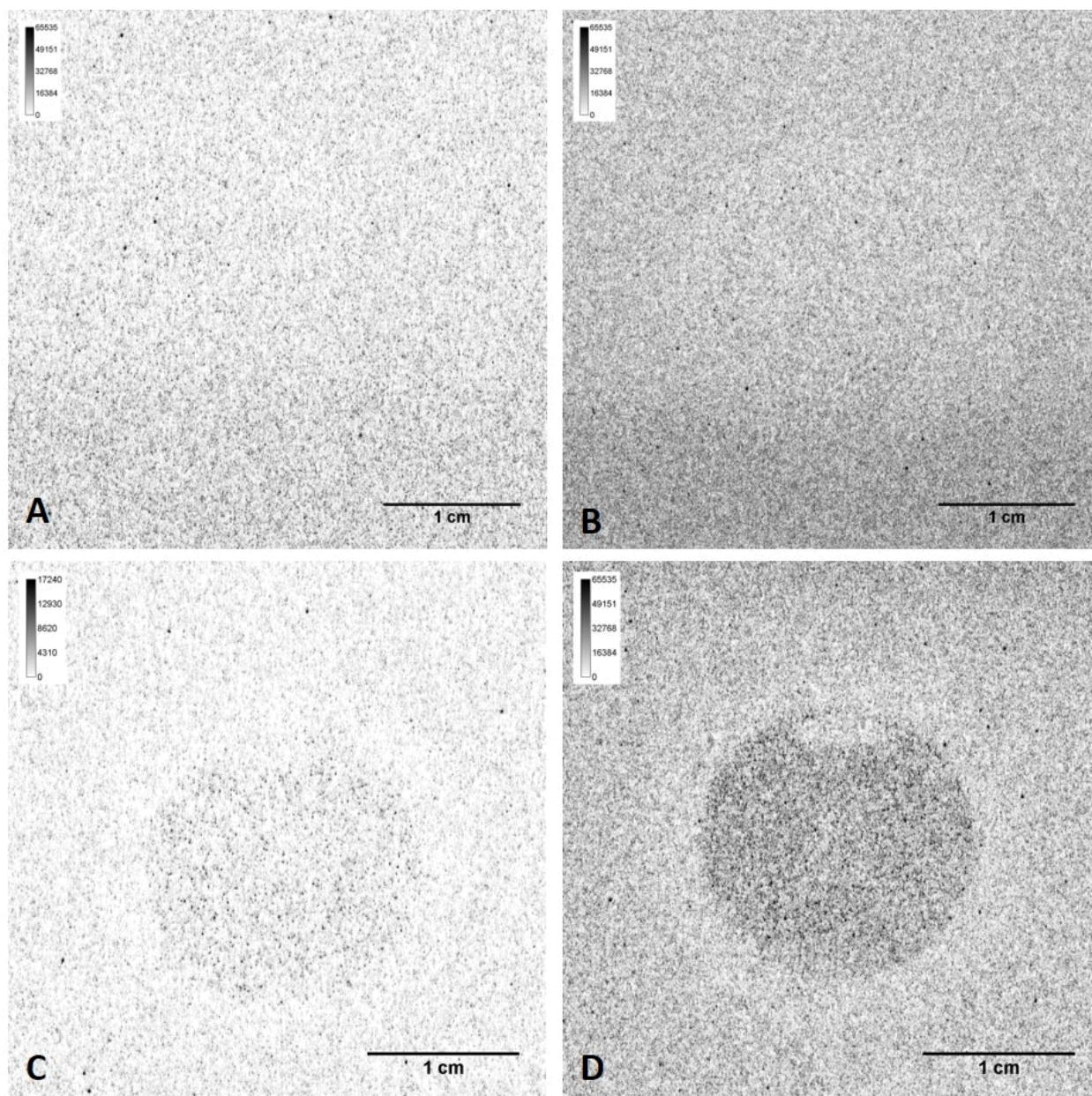


Figure 3. Autoradiographs obtained from low-activity uranium sources on SR image plates, using the maximum scan voltage of 1000 V: A) $3.69\text{E-}5 \text{ Bq/mm}^2$ ($3.06\text{E}12 \text{ atoms U/mm}^2$) exposed 24 hours, B) $3.69\text{E-}5 \text{ Bq/mm}^2$ ($3.06\text{E}12 \text{ atoms U/mm}^2$) exposed 120 hours, C) $3.69\text{E-}4 \text{ Bq/mm}^2$ ($3.06\text{E}13 \text{ atoms U/mm}^2$) exposed 24 hours, and D) $3.69\text{E-}4 \text{ Bq/mm}^2$ ($3.06\text{E}13 \text{ atoms U/mm}^2$) exposed 120 hours. Darker areas are the higher activity areas, and the contrast was artificially increased in Image J for visual clarity. In image A, the source activity is not detected because the activity density is below the background radiation levels. After 120 hours exposure (image B) background radiation levels continued to exceed the source activity density, and the IP area that was partially shielded by the stainless-steel disk source appears lighter in the autoradiograph. Both A and B have darker areas at the bottom that were completely unshielded, while the small Pb weight used to hold the IP in place provided some shielding in the rest of the image. The source with $3.69\text{E-}4 \text{ Bq/mm}^2$ produced a latent image with 24 hours exposure (C), and a clearer, higher intensity image after 120 hours exposure (D), as the activity flux exceeded background conditions.

Image resolution

The smallest available pixel size in the Typhoon FLA 7000 phosphorimaging system is 25 μm , but the best obtainable image resolution using the SR IPs is approximately 50 μm . This optimal resolution can generally be achieved with pure alpha emitters, in 2-dimensional samples polished very smooth and held in direct contact with the IP during exposure. Energetic beta particles have a longer range in the emulsion and may scatter erratically to create a lower resolution image. The two parameters that can be controlled to optimize image resolution are meticulous sample preparation, and avoidance of motion or vibrations during exposure. It is important to remember that spatial resolution is slightly diminished when the sample is not imaged in direct contact with the IP, and the image will be larger than the radioactive surface.

Film autoradiography requires long exposures in complete darkness, followed by chemical development. However, fine-grain films can produce autoradiographs with spatial resolution of approximately 10 μm . We tested the more traditional silver halide X-ray film-based method to establish relative resolution in comparison with the IP phosphorimaging method using historical nuclear fallout samples (Figure 4). Samples were prepared as polished glasses mounted in epoxy. Film autoradiography was performed using Agfa D3 single and double-sided emulsion X-ray film, held firmly in place on a traditional photographic 4x5 film holder, inside a Harrison 1000 light-tight Pup tent, with samples placed on top. After the end of the autoradiography exposure, the films were developed in 1:100 dilution Agfa Adonal developer, at 24°C for 9 minutes in a JOBO ATL-1500 automated drum processor. Following development and drying, X-ray films were scanned using a PDS Perkin Elmer microdensitometer. Slit width, or the size of the imaged area, was set to 10 μm and step size set to 3 μm .

Figure 4 shows autoradiographs of the glassy particle cross-section collected via 72 hours exposure to silver halide film (Fig. 3, left) or by 10.9 hours exposure to a TR IP (Fig. 4, right), scanned with 25 μm pixel size on a Fujifilm FLA-7000 scanner, with sensitivity setting S4000 (similar to 626 V PMT voltage on GE Typhoon 7000 that was used for other examples presented in this paper).. The film imaging conditions were optimized for spatial resolution, and image produced shows the distribution of radioactivity at the 10 μm scale. The IP imaging conditions were optimized for sensitivity and speed, and a general sense of the radioactivity distribution was achieved in approximately 1/6 of the exposure time required for film. Higher resolution autoradiographs were obtained using silver halide film instead of phosphorimaging, but at the expense of sensitivity and convenience. The TR IP are optimized for sensitivity to low-energy beta particles, but are otherwise similar to MS IPs, with a resolution of ~ 100 μm . We use SR IPs for most types of samples, as a middle-ground option that produces high-quality images with ~ 50 μm spatial resolution, but is less labor and time-intensive than film autoradiography. For nuclear forensic applications autoradiography is generally used as a screening technique, so the higher resolution of film autoradiography is not worth the additional exposure time needed, which would delay further analysis of the sample.

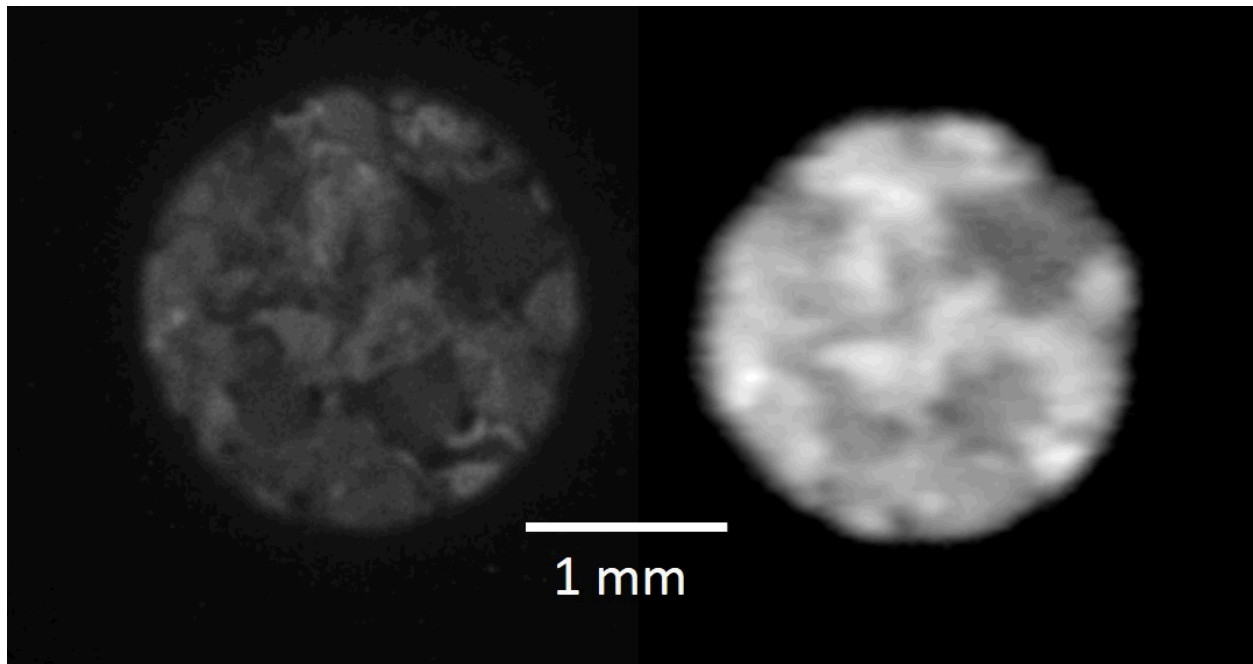


Figure 4: A comparison of autoradiographs from a cross-section of a piece of glassy historical fallout, collected at 72 hours exposure to silver halide film (left), and 10.9 hours exposure to a TR IP (right) scanned at S4000 setting on a Fujifilm FLA-7000 scanner. The film imaging conditions were optimized for spatial resolution, and image produced shows the distribution of radioactivity at the 10 μm scale. The phosphorimaging parameters were selected for sensitivity, and spatial resolution is limited to $\sim 100 \mu\text{m}$. The relative intensity scale is from low (black) to high (white).

Examples of nuclear forensic characterization applications

Autoradiography has previously been applied to monitor heterogeneity in mixed-oxide fuels for quality control purposes,^{34,35} and to study irradiated nuclear fuels.^{36–38} We have evaluated this approach as an early step in forensic analysis. Nuclear forensics laboratories encounter a wide variety of solid uranium-bearing samples related to the nuclear fuel cycle, such as fuel rods, pellets and plates. Spatially resolved analyses are often necessary for understanding the material properties and intended use. The bulk isotopic composition is measured by gamma spectrometry, but some types of fuel are heterogeneous and samples may even contain more than one source of uranium, each having different enrichments. Autoradiography characterizes activity heterogeneity in materials, and provide relative and qualitative clues about a material. For example, the radioactivity of unirradiated U fuel is generally correlated with enrichment. Other properties can also influence the radioactivity of U materials, such as U concentration, age, and irradiation history. Heterogeneous distribution of uranium in a sample or the presence of multiple enrichments of uranium is easily detected, provided the grains are larger than $\sim 50 \mu\text{m}$ (the spatial resolution of the technique).

Figure 5 shows an optical image and autoradiograph of the cross section from a high enriched uranium (HEU) fuel rod, collected with a 510 V scan (corresponding to S1000 Fuji setting) of the SR plate after 48 hours of sample exposure. The variation in image intensity shows that the fuel is heterogeneous at the 10-100 μm scale. Later SEM analyses confirmed that the fuel meat is composed of an Al-oxide matrix with chips of U-Al alloy, irregularly shaped and $\sim 10\text{-}50\ \mu\text{m}$ in size, incorporated in random orientations. Figure 6 shows optical image and autoradiograph of two low enriched uranium fuel pellet pieces, which were polished and embedded into a nano-SIMS sample holder prior to being exposed to an SR IP for 115 hours. These samples were composed of UO_2 and show relatively homogenous distribution of radioactivity. The higher relative activity of the left sample observed in the autoradiograph was consistent with later analyses confirming its slightly higher enrichment of ^{235}U and ^{234}U .

We recently demonstrated the utility of autoradiography for material characterization in a nuclear forensic investigation during the International Technical Working Group (ITWG) Collaborative Materials Exercise, CMX-5. For this exercise, participants were given samples of two low-enriched UO_2 pellets and tasked with developing and implementing an analytical plan to identify similarities and differences between the two samples, and answer specific questions injected by law enforcement. The samples were sub-aliquoted for a myriad of analytical techniques to be applied, and two of the sub-aliquots were sawed 10-10.5 mm long slices that were used for X-ray diffraction, then mounted and polished for spatial analyses. Figure 7 shows the mounted, polished CMX-5 samples 1 and 2, which were imaged by autoradiography prior to carbon coating for analysis by electron microscopy, nano-SIMS, and electron microprobe elemental analysis. The samples were held in contact with an SR image plate for 25 hours, via the exposure box described above, and the IP was scanned by the FLA 7000 in phosphorimaging mode at 626 V. The autoradiographs (Figure 8) immediately suggested that the isotopic enrichment of U in sample 2 was heterogeneous on the 50-100 μm scale, while sample 1 appeared to have roughly homogeneous distribution on the same scale. The mean image intensities over the two samples were similar, just as bulk isotopic data extracted from gamma spectra were similar, suggesting that the two samples may have been composed from mixtures of the same raw materials, but processed in ways that resulted in different sized domains of isotopically enriched U. After the exercise concluded, it was revealed that both samples were manufactured by mixing the same depleted U and low-enriched U materials via the Integral Dry Route at AREVA FBFC-Romans.³⁹ The differences in scale of heterogeneity occurred because sample 1 was manufactured with normal double cycle processing, where compaction occurs at low pressure, while sample 2 was produced via the inverse double cycle method, with high-pressure compaction. The ability to view the large picture of sample heterogeneity through autoradiography was complementary to the higher-resolution imaging of U isotopics via nano-SIMS, which focused on sub- mm^2 areas of the samples. Those results showed heterogeneity in sample 1 at the 1 to 10 μm scale, but the nature of heterogeneity in sample 2 was unclear. The autoradiograph from sample 2 was converted to a threshold image (Figure 9) which shows 131 areas of higher image intensity (top 9%), all with the same intensity. These high-intensity domains, caused by enriched U in the sample, ranged in area from $.0006\ \text{mm}^2$ to $0.7\ \text{mm}^2$.

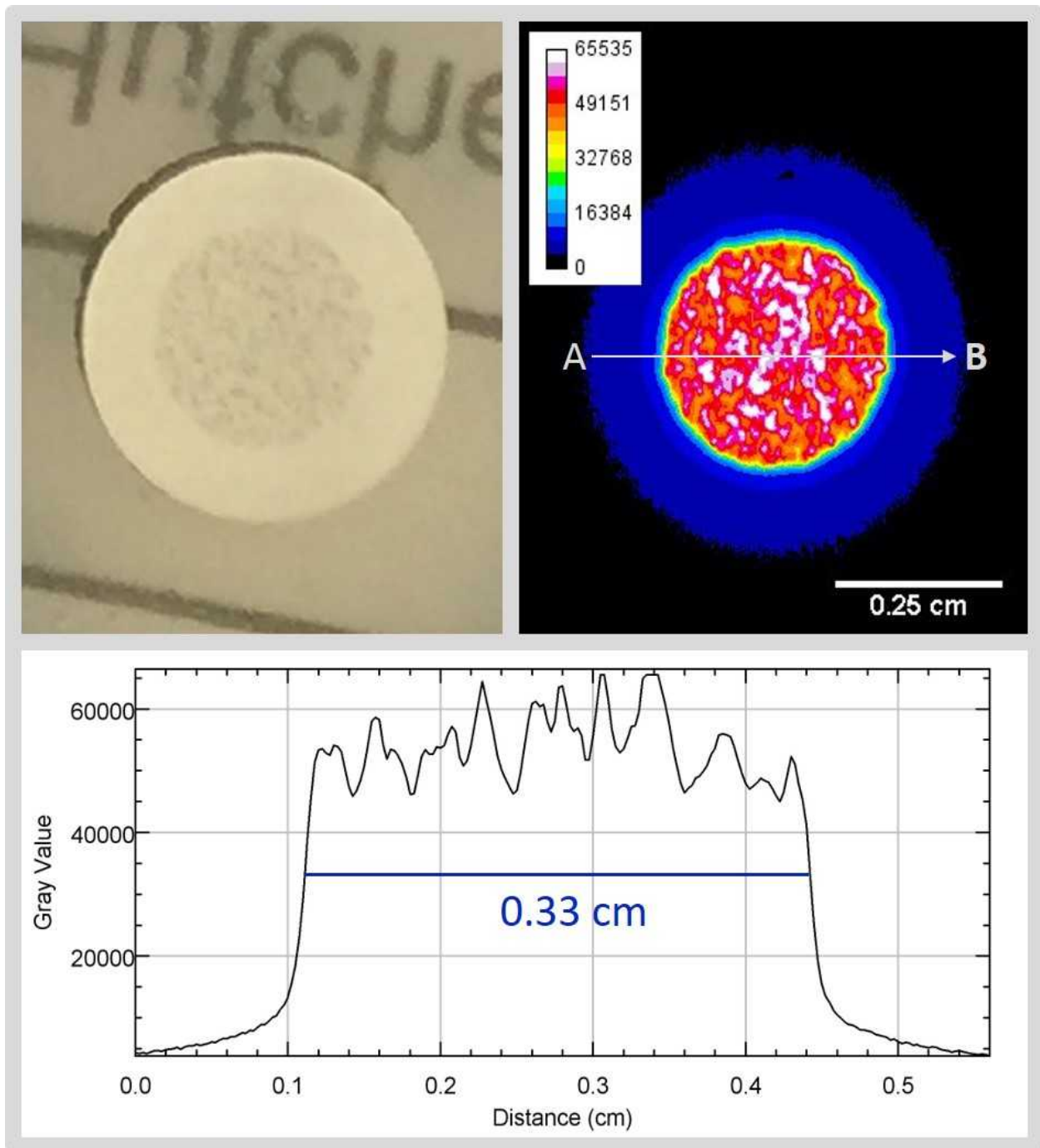


Figure 5: Optical image (top left) and autoradiograph (top right) of a cross section from a high enriched uranium fuel rod in Al cladding. The autoradiograph is from the second 510 V scan of an SR IP after 48 hours exposure to the sample. Heterogeneous distribution of fuel can be observed as variations in image intensity in the autoradiograph, where each pixel corresponds to 25 μm . Later scanning electron microscopy revealed that material fuel consisted of chips of U-Al alloy, randomly distributed in an aluminum oxide matrix. The lower plot shows the profile of raw image intensity (Gray Value) across the autoradiograph from point A to point B, with a steep change in intensity at the boundaries between the cladding and the fuel meat.

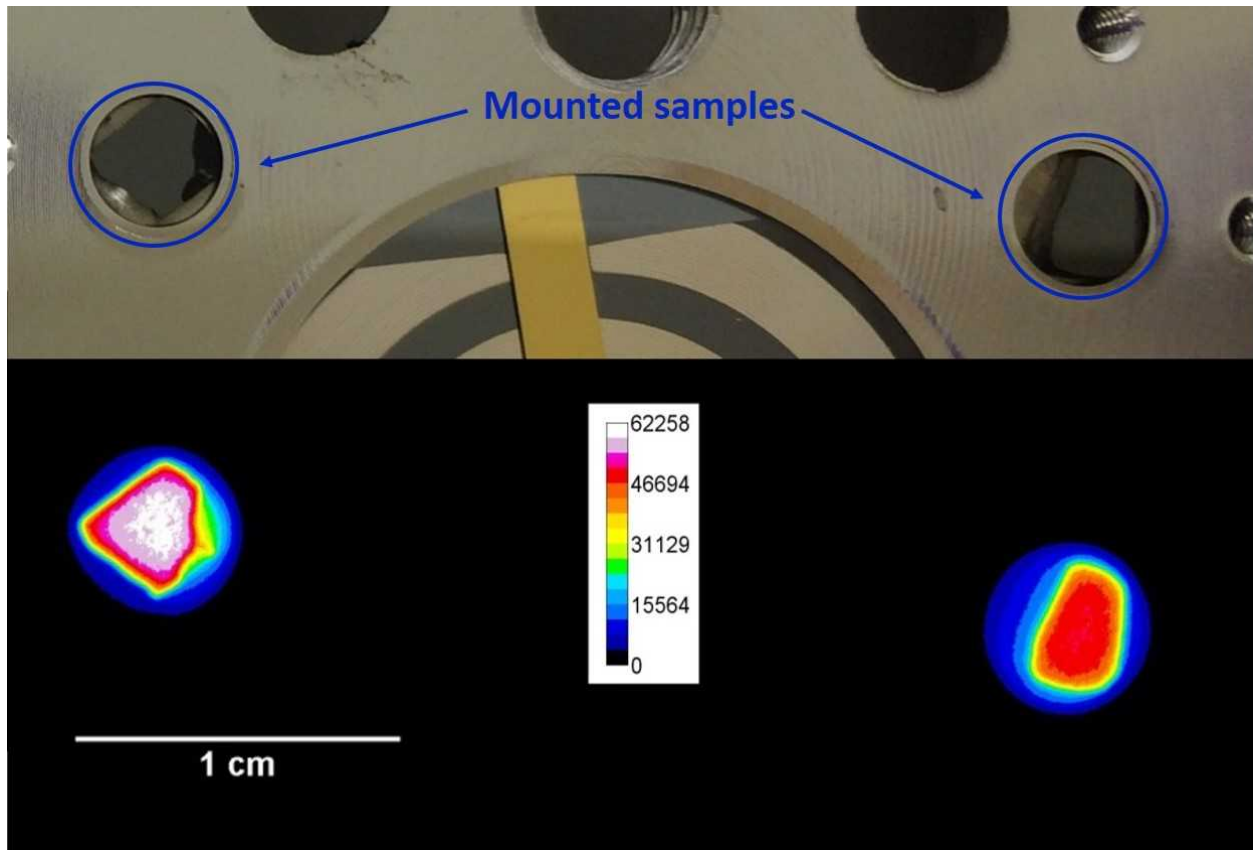


Figure 6: Optical image (top) and autoradiograph (bottom) of two low enriched uranium fuel pellet pieces, which were polished and embedded into a sample holder before being exposed to an SR IP for 115 hours. The IP was scanned with 510 V, with pixel size 25 μm . The image demonstrates general homogeneity in the distribution of activity within in both samples, but shows that the samples are not the same. The relative intensity of the two samples suggests higher uranium enrichment in the left sample compared to the right sample.

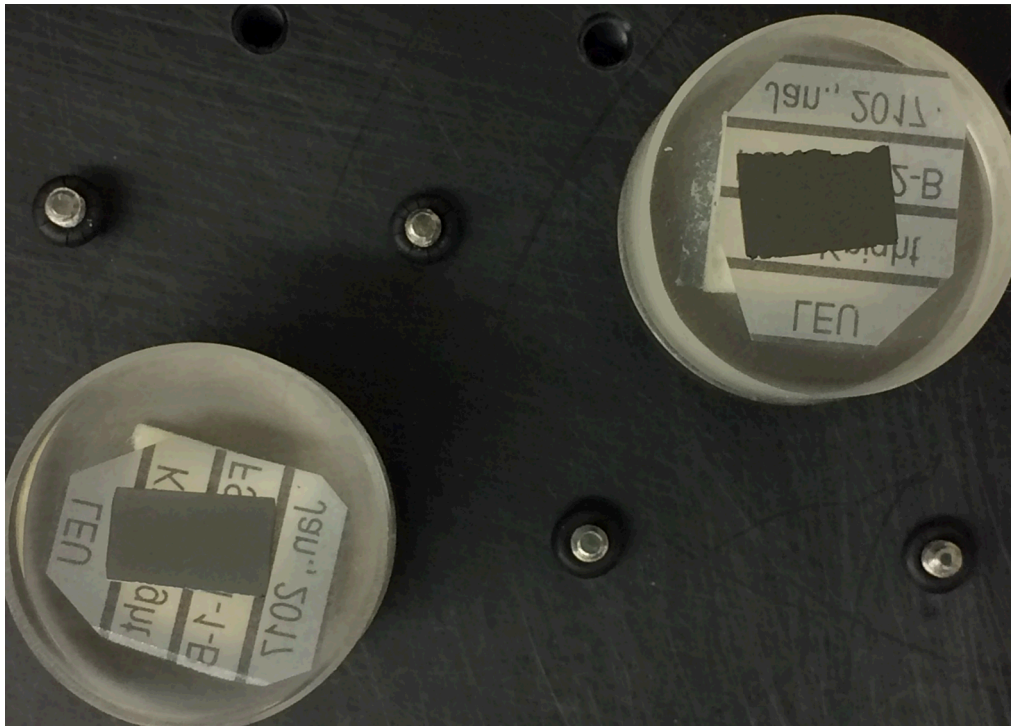


Figure 7: Polished slices of low-enriched UO_2 samples for CMX-5 exercise, CMX-5 sample 1 (left) and CMX-5 sample 2 (right), mounted for autoradiography.

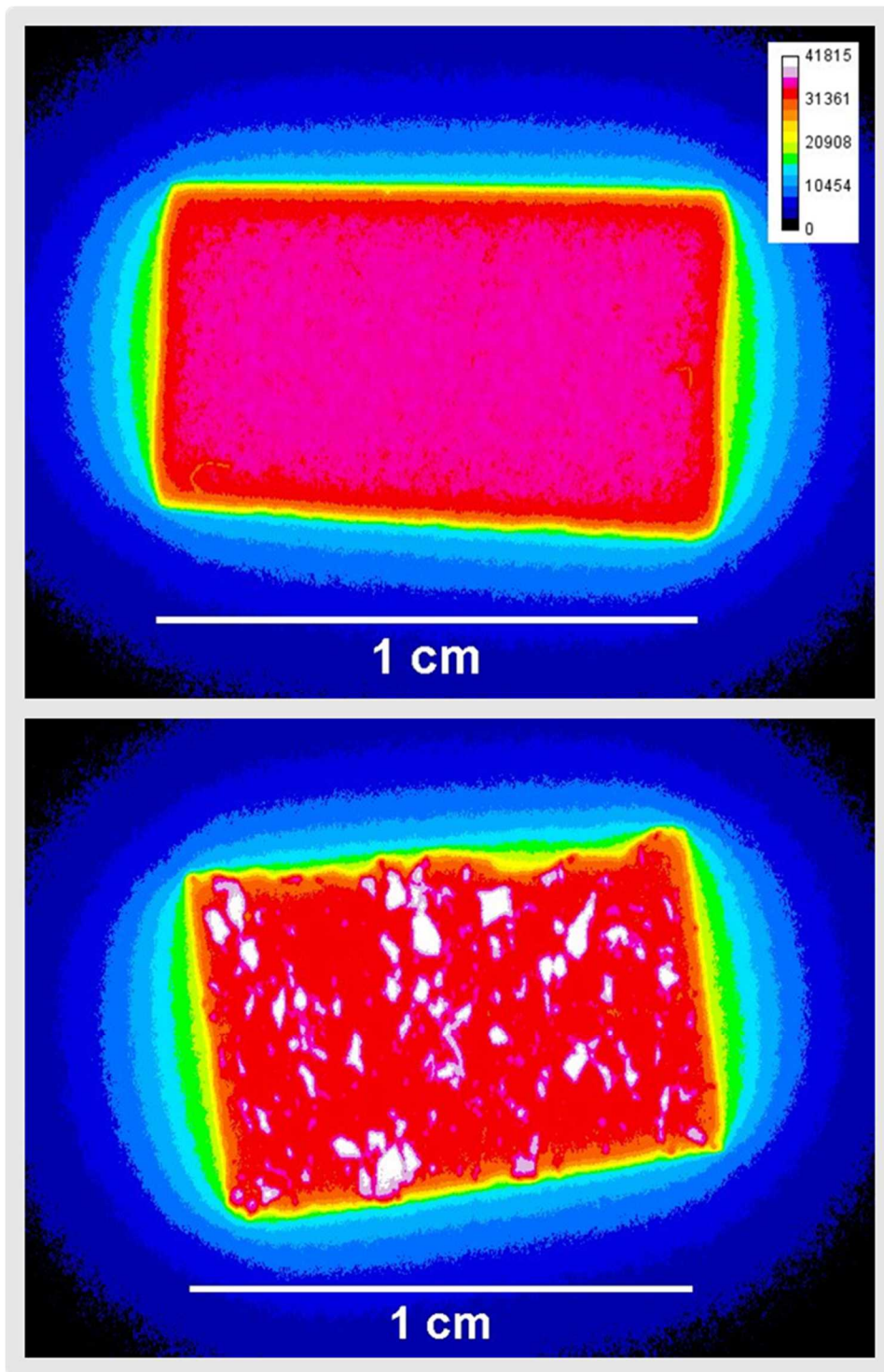


Figure 8: Cropped autoradiographs of the sawed low enriched UO_2 sub-aliquots, CMX-5 sample 1 (top) and CMX-5 sample 2 (bottom) which were mounted in epoxy and polished before being exposed to an SR IP for 25 hours. The IP was scanned with 626 V, pixel size 25 μm . Sample 2 is characterized by heterogeneity, on the 50-100 μm scale, in the distribution of activity, while sample 1 shows a roughly homogenous distribution on the same scale.

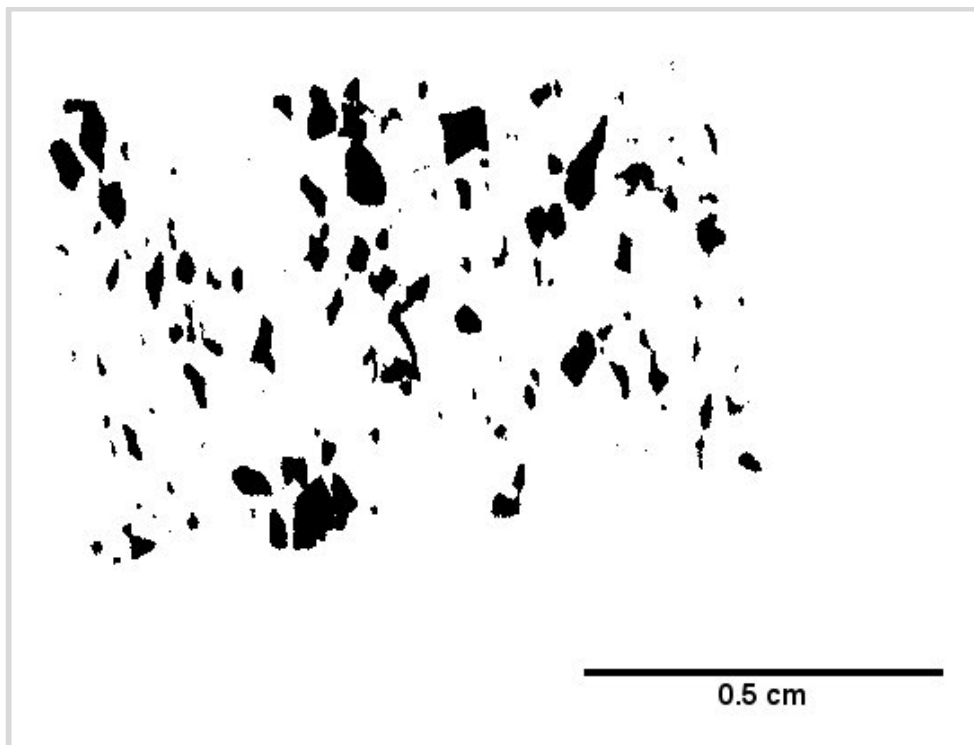


Figure 9: Threshold image CMK-5 sample 2, showing only pixels exceeding raw image intensity value of 36126, the top 9% of pixels, all with the same intensity. The high-intensity regions exceeding the threshold range in area between 0.0006 mm^2 and 0.7 mm^2 , and were caused by domains of UO_2 in the sample that are enriched to approximately 4.2% ^{235}U .

Conclusions

Digital autoradiography has been incorporated as part of a comprehensive suite of analytical techniques applied to nuclear forensic analysis of solid materials. Autoradiography is an excellent qualitative technique for surveying the distribution of radioactivity in samples to establish scales of activity heterogeneity, and to identify areas of interest for further microanalysis. Although autoradiography is relatively simple and low-cost, and generally non-destructive, best results are achieved with careful sample preparation and properly controlled exposure conditions. Imaging plates have high sensitivity to ionizing radiation, a wide dynamic range, and can characterize even large surfaces quickly and easily.

Image-plate autoradiography has been applied to nuclear forensics as a qualitative, or semi-quantitative technique by which to compare relative α and β activities in different areas of a sample, or multiple samples imaged together. The extraction of quantitative information from autoradiographs is often limited by convolution of excitations caused from multiple radionuclides close in space. Silver halide film autoradiography may be applied to maximize spatial resolution at the expense of sensitivity and convenience, but requires longer exposures and chemical post-processing. Developments in the biomedical imaging industry have also improved the spatial resolution and spectral deconvolution available in digital autoradiography.⁴⁰ Autoradiography is a valuable tool for nuclear and radioactive material characterization, and will continue to be applied to problems of nuclear forensics in the future.

Acknowledgements

This document, LLNL-JRNL- 735865 was prepared by LLNL under Contract DE-AC52-07NA27344. TPD thanks the Department of Homeland Security National Technical Nuclear Forensics Center postdoctoral fellowship (LLNL.15.010.A) for funding. The authors would like to thank Dave Ruddle of LLNL for engineering support, and former LLNL summer intern Anna Lindquist for early development assistance.

References

- (1) Rogers, A. *Techniques of Autoradiography*, 3rd ed.; Elsevier/North-Holland biomedical Press, 1979.
- (2) J.H. Webb. *Phys. Rev.* **1948**, 74 (5), 511–541.
- (3) Sonoda, M.; Takano, M.; Miyahara, J.; Kato, H. *Radiology* **1983**, 148 (3), 833–838.
- (4) Amemiya, Y.; Miyahara, J. *Nature* **1988**, 336 (3), 403–405.
- (5) Iwabuchi, Y.; Umemoto, C.; Takahashi, K.; Shionoya, S. *J. Lumin.* **1991**, 48–49, 481–484.
- (6) Solon, E. G. *Expert Opin. Drug Discov.* **2007**, 2 (4), 503–514.
- (7) Pilgrim, C.; Stumpf, W. E. *J. Histochem. Cytochem.* **1987**, 35 (8), 917–928.
- (8) Dugger, W. M. *Bot. Rev.* **1957**, 23 (6), 351–387.
- (9) Goodman, C.; Picton, D. C. *Phys. Rev.* **1941**, 60 (9), 688.
- (10) Yegooa, H. *Am. Mineral.* **1946**, 31 (3 & 4), 87–124.
- (11) Faruqi, A. R. *Nucl. Instruments Methods Phys. Res. Sect. A-Accelerators Spectrometers Detect. ASSociated Equip.* **1991**, 310 (1–2), 14–23.
- (12) Bienz, K. A. *Microsc. Acta* **1977**, 79 (1), 1–22.
- (13) Pelc, S. R. *J. R. Microsc. Soc.* **1963**, 81 (3 & 4), 131–139.
- (14) Adams, C. E.; O'Connor, J. D. *The Nature of Individual Radioactive Particles VI. Fallout Particles From a Tower Shot, Operation Redwing*; 1957.
- (15) Adams, C. E.; Farlow, N. H.; Schell, W. R. *Geochim. Cosmochim. Acta* **1960**, 18 (1–2), 42–56.
- (16) Fahey, A. J.; Zeissler, C. J.; Newbury, D. E.; Davis, J.; Lindstrom, R. M. *PNAS* **2010**, 107 (47), 20207–20212.
- (17) Belloni, F.; Himbert, J.; Marzocchi, O.; Romanello, V. *J. Environ. Radioact.* **2011**, 102 (9), 852–862.
- (18) Wallace, C.; Bellucci, J. J.; Koeman, E. C.; Burns, P. C. *J. Radioanal. Nucl. Chem.* **2013**, 298, 993–1003.

- (19) Lewis, L. A.; Knight, K. B.; Matzel, J. E.; Prussin, S. G.; Zimmer, M. M.; Kinman, W. S.; Ryerson, F. J.; Hutcheon, I. D. *J. Environ. Radioact.* **2015**, *148*, 183–195.
- (20) Kristo, M. J.; Gaffney, A. M.; Marks, N.; Knight, K.; Cassata, W. S.; Hutcheon, I. D. *Annu. Rev. Earth Planet. Sci.* **2016**, *44*, 555–582.
- (21) Hutcheon, I. D.; Grant, P.M.; Moody, K. J. In *Handbook of Nuclear Chemistry, Vol. 1*; Vertes, Attila; Nagy, Sandor; Klencsar, Zoltan; Lovas, Rezso G.; Rosch, F., Ed.; Springer, 2011; pp 2837–2891.
- (22) Chung, B. W.; Erler, R. G.; Teslich, N. E. *J. Nucl. Mater.* **2016**, *473*, 264–271.
- (23) Stefaniak, E. A.; Darchuk, L.; Sapundjiev, D.; Kips, R.; Aregbe, Y.; Van Grieken, R. *J. Mol. Struct.* **2013**, *1040*, 206–212.
- (24) Mukai, H.; Hatta, T.; Kitazawa, H.; Yamada, H.; Yaita, T.; Kogure, T. *Environ. Sci. Technol.* **2014**, *48*, 13053–13059.
- (25) Parker, W.; Bildstein, H.; Getoff, N. *Nucl. Instruments Methods* **1964**, *26*, 55–60.
- (26) Bajo, S.; Eikenberg, J. *J. Radioanal. Nucl. Chem.* **1999**, *242* (3), 745–751.
- (27) Ramm, P. *J. Neurosci. Methods* **1994**, *54*, 131–149.
- (28) Williams, G. J.; Maddox, B. R.; Chen, H.; Kojima, S.; Millecchia, M. *Rev. Sci. Instrum.* **2014**, *85* (11), 11E604.
- (29) Zeissler, C. J.; Wight, S. A.; Lindstrom, M. **1998**, *49* (9), 1091–1097.
- (30) Zeissler, C. J.; Lindstrom, A. P. *Nucl. Instruments Methods Phys. Res. Sect. A Accel. Spectrometers, Detect. Assoc. Equip.* **2010**, *624* (1), 92–100.
- (31) Chen, B.; Zhuo, W.; Kong, Y. **2011**, *46*, 371–374.
- (32) Takebe, M.; Abe, K. *Nucl. Instruments Methods Phys. Res. A* **1994**, *345*, 606–608.
- (33) Takebe, M.; Abe, K.; Manaba, S.; Yoshiyuki, S.; Yasuhiro, K. *Nucl. Instruments Methods Phys. Res. A* **1995**, *359*, 625–627.
- (34) Baghra, C.; Sathe, D. B.; Sharma, J.; Walinjar, N.; Behere, P. G.; Afzal, M.; Kumar, A. *J. Nucl. Mater.* **2015**, *467*, 730–741.
- (35) Shriwastwa, B.; Raghunath, B.; Ghosh, J. *Kerntechnik* **1992**, *57* (5), 283–285.
- (36) KleyKamp, H.; Pejsa, R. *J. Nucl. Mater.* **1987**, *75* (2), 297–300.
- (37) Gruber, W. *Trans. Am. Nucl. Soc.* **1969**, *12* (2), 842.
- (38) Nauche, R. *Euro-Spectra* **1969**, *8* (3), 87.
- (39) Beauvy, M.; Berthoud, G.; Defranceschi, M.; Ducros, G.; Guérin, Y.; Limoge, Y.; Madic, C. *Nuclear fuels*; 2009.
- (40) Riou, L.; Inerm, E.; Animage, C. L.; Broisat, A.; Ghezzi, C.; Inerm, E. *SIMULTANEOUS DUAL-*

ISOTOPE IMAGING OF TECHNETIUM-99m AND THALLIUM-201 USING THE BETAIMAGER™ D FINE SYSTEM • Simultaneous imaging of two different radiolabeled tracers in myocardial slices • Quantitative comparison of uptake of a 2 given radiolabeled flow; 2011.